Turbulence Measurements in a Radial Upwash

Barry Gilbert*
Grumman Corporate Research Center, Bethpage, New York

Results are presented of an experimental investigation of the abnormally high turbulent-mixing-layer growth rate characteristics found in the upwash regions of V/STOL flows near the ground. Experiments were performed in a unique radial wall jet facility to examine the structure of the upwash and provide quantitative estimates of the momentum distribution and entrainment. The unique aspect of the configuration is that the radial wall jets are formed by impinging circular jets coming from below the ground plane onto deflector plates, forming a flow that contains the essential characteristics of a radial upwash while decoupling the problem caused by the impinging jets on the ground plane and recirculation zone. Radial wall jet measurements verified traditional values established for mixing-layer growth and mean velocity decay. Parameters used to characterize the upwash formation were identified as the maximum wall jet velocity and the wall jet half-velocity width. The increased mixing-layer growth rate was larger than a free jet by a factor of two. This is explained by the much larger eddies and intermittency caused by the head-on collision process at the point where the upwash forms. The time-averaged turbulence level was found to be only about 10% higher than that found in the free jet.

Introduction

A UNIQUE turbulent mixing phenomenon results from the collision of opposing wall jets. The mean velocity profile of the generated flow appears to be similar to those found in free jet turbulent flows. However, the macroscopic properties of mixing-layer growth rate and the corresponding mean velocity decay rate are significantly different. This combined effect means that there is a different distribution of average momentum in the flow.

One such flow recently has been identified due to the development of aircraft with V/STOL capability. When a V/STOL aircraft is near the ground, the exhaust from the aircraft lift jets interacts with the ground, producing an upwash flow directed toward the underside of the aircraft. An understanding of the basic physical mechanisms acting in the flowfield between the aircraft and the ground is vital to the successful development of a practical V/STOL aircraft.

The upwash flow is very difficult to analyze because of the much greater mixing-layer growth rate when compared to other types of turbulent flows.[1-7] The problem is made computationally difficult by the intrinsic three-dimensionality of the upwash and because the turbulence in this type of flow is not understood. Although the upwash flowfield is very complex, the analysis that is most often used is based on a simple model. The mean velocity profile in the upwash along a line connecting the source wall jets looks like the profile found in a radial free jet. A simple momentum balance along the collision line requires the formation of a fan in the symmetry plane between the to jets (see Fig. 1). Extrapolating these velocity vectors back to their virtual origin is equivalent to folding down the ground plane. The flow then is analyzed simply as a radial free jet with its origin located at the impingement point of the source jets. This works fine in the symmetry plane. The most obvious problem with this type of analysis is due to the much faster growth rate found in the upwash compared to a free jet. This accelerated growth rate influences both the distribution of momentum in the upwash, producing additional lift, and the magnitude of the entrainment field, contributing to the suckdown on the aircraft. As diagrammed in Fig. 1, the real upwash fan extends over a much broader region than the free radial upwash model predicts.

In this experimental program, detailed measurements were taken in the upwash flow created by the collision of radially flowing wall jets. This configuration closely approximates the actual V/STOL flow behavior. Three velocity components and several higher moments that appear in the turbulent kinetic energy equations as well as length scale and intermittency measurements were made. Measurements were taken along the axis connecting the two source jets as well as off this axis at six heights above the ground. Experiments conducted with a two-dimensional upwash have been reported previously.[8,9] Complete radial data may be found in Refs. 10 and 11. In this paper, we report on the mixing-layer spread rate and the mean velocity decay rate in the upwash fan. We show the nondimensional profiles using the pertinent scaling parameters of the flow.

Apparatus and Instrumentation

A new wind tunnel facility was designed and constructed for the study of the upwash created from the collision of radially flowing wall jets. The usual method employed for the generation of this sort of wall jet is the impingement of a circular free jet into a ground plane. Although this method undoubtedly creates a radial wall jet, in the case of an upwash, it also introduces an additional complication. It is impossible to isolate the effects of the presence of circular free jets on the development of the upwash physically located between them. The downward-flowing free jets set up a strongly coupled, secondary rotating flow with the upward-flowing upwash. This coupled effect will be examined in a later study.

We wanted to generate a highly controllable upwash flow whose characteristics would not be affected by the presence of a large secondary flow. The method chosen to create the radial wall jet was one that employed a circular source jet flowing

Presented as Paper 87-1435 at the AIAA 19th Fluid Dynamics, Plasma Dynamics and Lasers Conference, Honolulu, HI, June 8-10, 1987; received June 19, 1987; revision received Feb. 11, 1988.

*Staff Scientist. Senior Member AIAA.

through the ground plane from below. The circular jet is diverted into the radial direction along the ground by impinging it on a circular deflector plate. By varying the deflector cap radius R and gap size G, it seems possible to generate any type of growth rate consistent with conservation laws. The geometry chosen was the one that gave the closest match of radial wall jet characteristics to those of a radial wall jet formed by an impinging jet.

The flow facility is shown in Fig. 2. The photograph shows the two source jets exhausting from the two independent plenum chambers below the instrumentation plate representing the ground plane. The deflecting plates are mounted by three support cantilevers with the gap spacing set by machined spacers. A circular disk is part of the instrumentation plate located between the source jets. It contains a series of eight static-pressure taps. By rotating this disk, the entire static-pressure field on the ground between the two source jets may be mapped. The gap height is 5 mm, and the deflection plate has a 15.25 cm diameter. The instrumentation plate is 100 cm × 50 cm, and the distance between the source radial jet exits is 35 cm or 70 gap heights. The radial jet exit velocity is typically 95.5 m/s.

The velocity data in the upwash were taken with a commercial X-probe hot-film anemometer calibrated in our facility. The experiment and data acquisition are controlled by our real-time minicomputer system. The anemometer signals were linearized. Two time series from the anemometers and various other flow conditions are taken at each point. The time series are preprocessed in real time and stored before the program increments the probe position. At each point, 32,768 data pairs are taken at 2500 pairs/s for about 13 s. This may seem to be too low a sampling rate for such a highly turbulent flow. However, using the characteristic length scale and velocity scale at the collision point gives a characteristic frequency of about 1000 Hz. Sampling here is more than twice that value. Further, measurements made with a nonintrusive laser Doppler anemometry give the same values as measured by the hot-film probes.

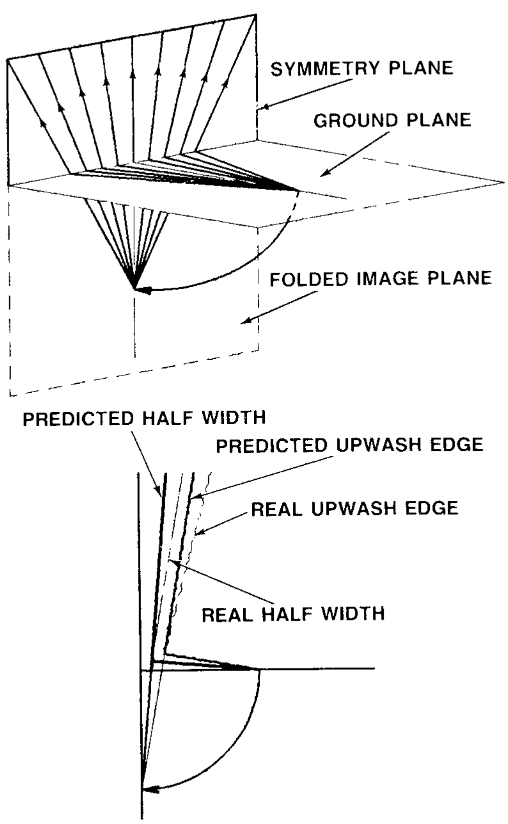

Fig. 1 Diagram showing current analysis using a folded image plane.

A smoke flow-visualization system was used to examine qualitatively the important features of the upwash flow. The system we developed used two sets of cylindrical lenses to form a thin laser sheet with variable height and width. A 2 = W Argon ion laser was used as a source. Two 256 mm focal-length cylindrical lenses were spaced nominally 100 mm apart. By adjusting the spacing, laser sheets from 2.5 to 25 cm in height could be formed to illuminate whatever flow features we want to examine. A second set of two 96 mm focal-length cylindrical lenses with axes oriented perpendicular to the first set allowed variation in the thickness and sharpness of the sheet. A spacing of about 100 mm gave a very intense sheet at all heights of approximately 1.5 mm thickness. The laser sheet was moved in space by traversing mirrors on a three-axis mechanism. The flow was seeded selectively with one or two smoke sources. The smoke was generated by vaporizing a biologically safe plant oil. The images were recorded on videotape, and photographs were taken from this tape using a digital frame grabber.

Wall Jets

The radial wall jets are the initial conditions for the upwash. As in any flow, the initial conditions have a tremendous, first-order effect on the flow. An upwash is particularly sensitive because it is generated by the head-on collision of wall jets, resulting in a stagnation flow with high pressure.

Figure 3 is a flow-visualization photograph of the radial wall jet that clearly shows the qualitative behavior expected in a turbulent radial wall jet. The flow is left to right, and the seeding is by entrainment with the smoke probe at the radial jet exit. This technique gave very good results. The linear growth of the wall jet can be seen. The dark wedge below the wall jet is the shadow of the right deflector plate in the laser sheet coming from the right. Note the eddy size and apparent intermittency.

Turbulent jet flows are characterized by their macroscopic properties of mixing-layer growth and mean velocity decay. The growth rate is defined by the physical length from the centerline, for a free jet, or from the wall, for a wall jet, to the point where the velocity has fallen off to half its maximum value. This is called the half-velocity height or width. The virtual origin is found by extrapolating the linear growth rate

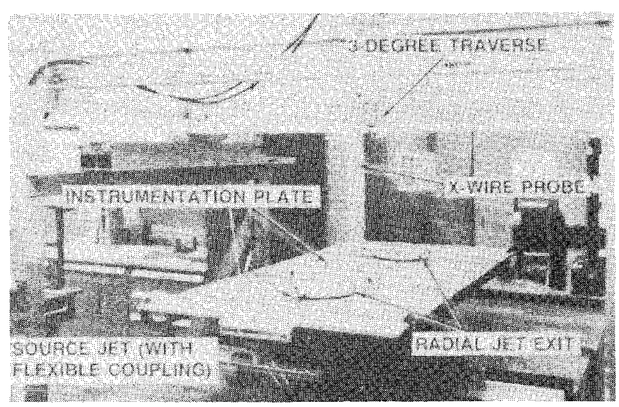

Fig. 2 Photograph of radial wall jet upwash facility.

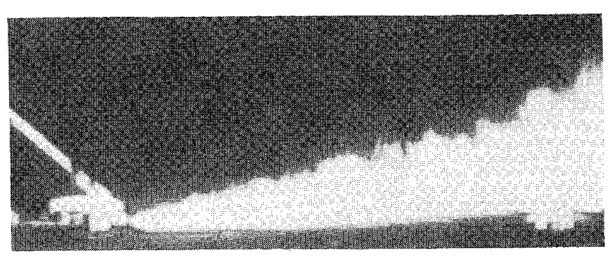

Fig. 3 Flow visualization photograph showing a single wall jet.

curve to a half-velocity height of zero. The decay rate is given by the decrease in maximum velocity with downstream distance. These two physical characteristics are related by conversation of momentum. For a radial wall jet, the conservation law requires a linear decay of the form $U \sim X^{-1}$.

Wall jet mean and turbulence profiles were taken at 16 locations from the radial jet exit to a position beyond the centerline in increments of approximately four gap heights. The data acquisition and movement of the single-element hot-film probe were controlled by the automatic digital data system. A plot of the wall jet growth rate as characterized by the half-velocity height vs the distance downstream is given in Fig. 4a for each wall jet. A linear least-squares curve fit of the data from stations 4 through 16 ($X_w/G > 14$ to 60) gives a growth rate of 0.097. The first stations were not used in the curve fit because they are in the developing region. This is slightly larger than the growth rate value for an axisymmetric wall jet (0.078) but is close to the value for radial wall jets produced by impinging circular free jets on a plate (0.087). The virtual origins, defined by the half-velocity growth curve, are -7.14 and -7.20 gap heights, which are about halfway between the center and outer edge of the deflector plates. Figure 4b shows the required linear decay of the maximum velocity vs distance.

Matching the maximum velocity values at the physical centerline alone was not enough to ensure that the upwash fan would form vertically. In early tests, the matched maximum velocity criterion produced an upwash fan that formed at the physical centerline but that was not vertical. Careful measurement of each velocity profile at the centerline showed that due to almost imperceptible variations in the nozzle exit geometry, one flow had an excess of momentum above the maximum velocity point. This caused the flow to slant away from that side, showing the strong sensitivity of the flow to very small differences in the velocity profile. The source wall jets were manipulated to give nearly identical momentum distributions at the collision point. The exit velocity was 95.5 m/s, which gives a Reynolds number based on jet velocity and nozzle gap height of 33×10^3.

The wall jet characteristics at the centerline ($X_w/G = 35$) when no collision occurs are used to normalize upwash data. At the centerline, the wall jet half-velocity height is $B_w = 4.0G = D = 20.50$ mm, and the characteristic velocity is $U_{c\ell} = 0.218 U_{\rm jet} = 20.8$ m/s. The value D is the characteristic height for the upwash. The collision region of influence extends to about $2D$. The upwash Reynolds number based on these centerline dimensions is 29×10^3. The distance between source jet virtual centers is $20.9D$.

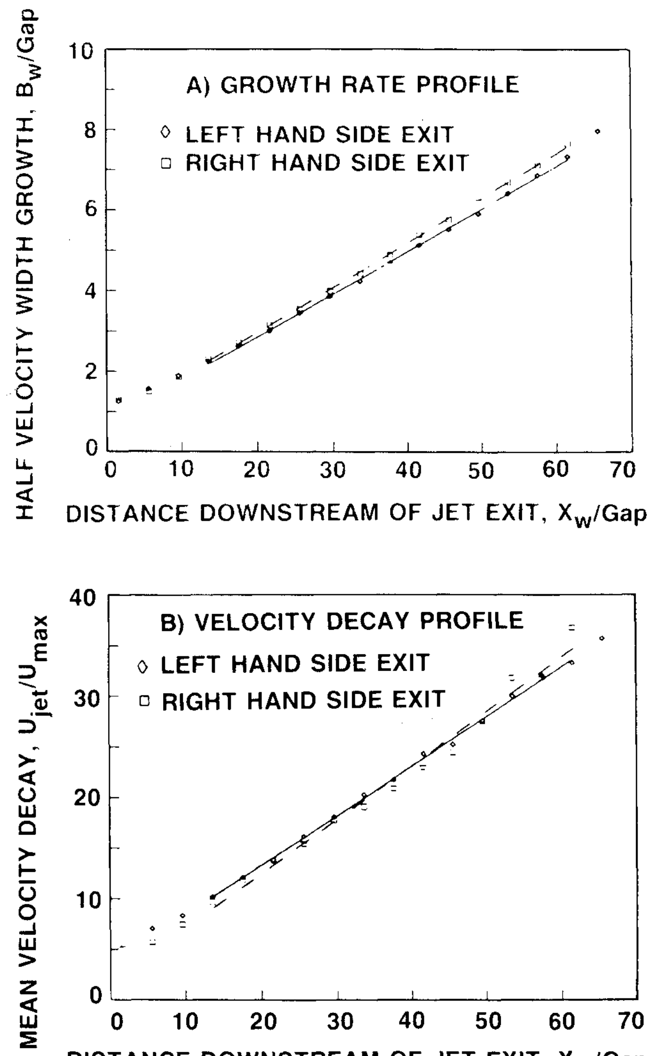

Fig. 4 Radial wall jet characteristics.

Upwash Measurements—Centerline

A good qualitative indication of what is happening in the upwash is obtained from the flow-visualization picture of the upwash. In Fig. 5, only the left jet is seeded, and so it is the only one visible. The radial wall jets collide at the centerline, creating the upwash. The presence of the right wall jet is clearly visible by its effect on the seeded jet. It appears that no flow emanating from the left passes through to the right-hand side of the upwash. Figure 5b shows this effect viewed from the top. The laser sheet was rotated 90 deg so that it illuminated a plane nearly parallel to the ground plane. The bright spots are primarily due to laser light reflections from solid structure. Since the seed is injected at a point, a radial pie slice shows up in the laser sheet. Because only one wall jet is seeded but both are running, the flow at the collision point turns abruptly vertical and moves out of the laser plane. No seed penetrates past the collision point at this height above ground. The full upwash is made visible in Fig. 6. The relative size of the eddies in the wall jet and the upwash is clearly seen. The less dense smoke outside the upwash structure shows the en-

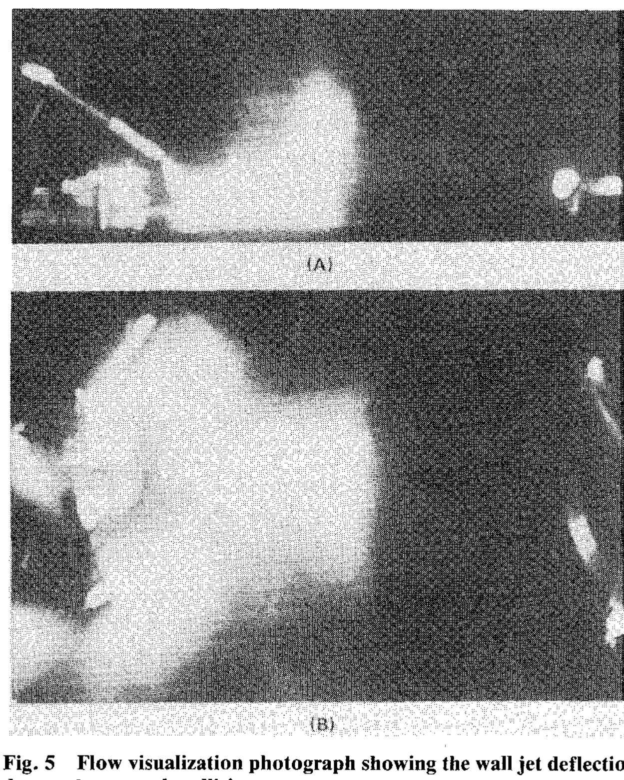

Fig. 5 Flow visualization photograph showing the wall jet deflection due to the upwash collision.

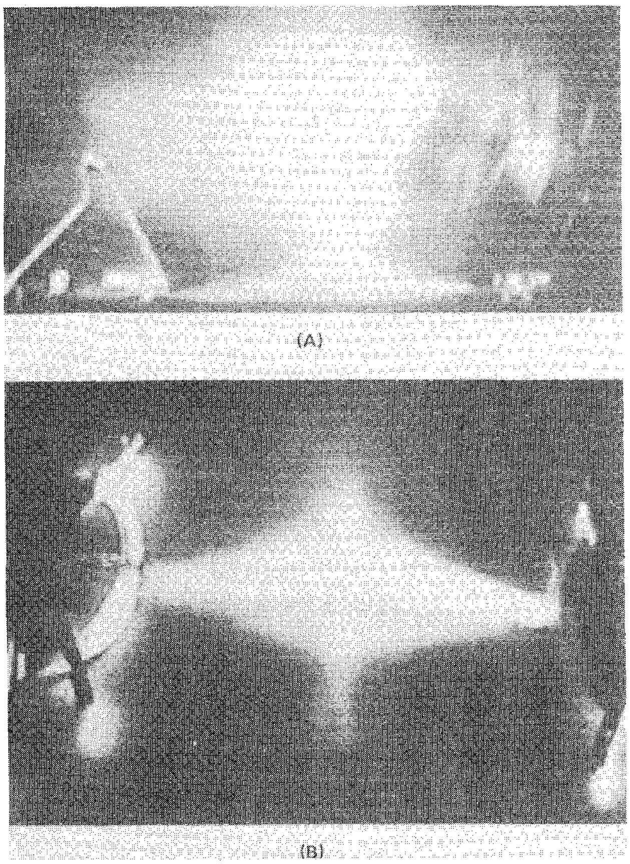

Fig. 6 Flow visualization photograph showing full upwash structure.

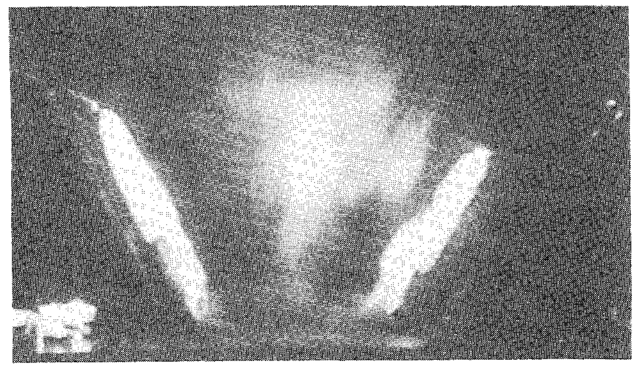

Fig. 7 Flow visualization photograph showing large entrainment (suckdown) flowfield.

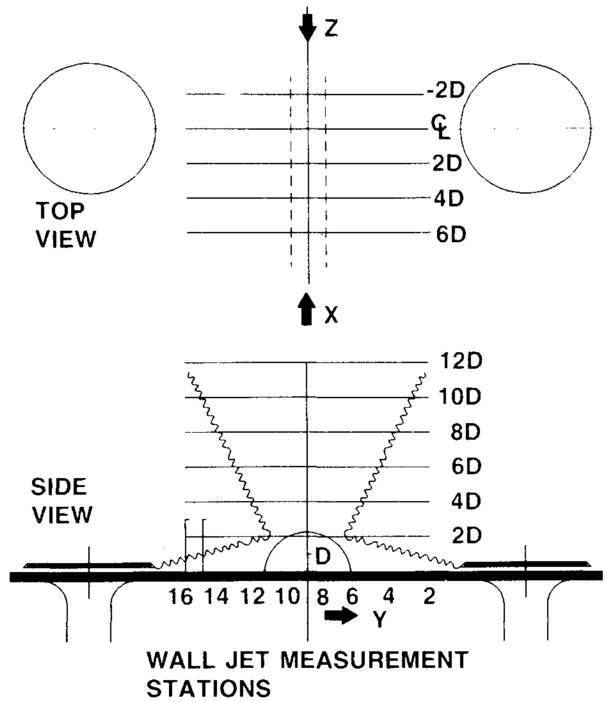

Fig. 8 Diagram showing measurement stations and coordinate system used.

trainment flow. Figure 6b shows the top view. Flow is strongly entrained ino the base of the upwash as seen by seeding the entrained flow in Fig. 7. The smoke is ejected from the probes with no velocity of its own. Therefore, the strong suckdown of the entrainment field is due to the presence of the upwash. This is significantly different from a free jet in which case the smoke would move upward with the jet, joining it nearly tangentially.

Figure 8 shows the location of the measurement stations in the upwash. The value D, the half-velocity height at the collision point of an individual radial wall jet, is the characteristic dimension of the upwash. Measurements were made along the centerline connecting the two jets at six heights from $2D$ to $12D$. Profiles also were taken at four cross-stream locations in the Z direction. These profiles at $2D$ increments were $6D$ to $-2D$ and at the same four lower heights as used for the centerline position. Additional profiles were taken along the Z plane in the symmetry plane and at one-half width to either side of the symmetry plane at heights of $4D$ and $6D$. Each profile contained 60 points positioned approximately $0.23D$ (4.8 mm) apart, except at the lowest station where they were at half that value. Each profile was repeated with the X probe rotated 90 deg so that all three velocity components at each point were measured. Since this procedure repeats the "U" measurement, it is a good check on the reproducibility of the data.

The mean velocity profiles in the upwash direction were curve-fitted with least-squares curve of the form $U = A + C \exp[-(Y - Y_0)^2/2S^2]$, where Y_0 is the symmetry coordinate, $A + C$ is the maximum velocity, and S may be used to define the half-velocity width as $B(U = U_{max}/2) = 1.177\ S$. This curve-fit procedure is superior to the usual determination of half-width that relies on interpolating between data points to find $U_{max}/2$. That method suffers severely from data scatter in both the determination of U_{max} and the interpolation at $U_{max}/2$, and it rarely gives symmetric half-velocity positions.

The half-velocity growth-rate curve defined by the curve-fit technique is shown in Fig. 9a. The growth rate shown is about 0.25. This value is essentially the same one found in the previous two-dimensional upwash (0.23) and is more than twice the free jet value (0.11). The mean velocity decay curve is shown in Fig. 9b. The data are plotted in a form to give the linear relationship required by conservation-of-momentum considerations.

The normalized mean velocity profiles at six heights are shown in Fig. 10. The profiles have been shifted to their symmetry point and normalized by the local half-velocity width and local maximum mean velocity as determined by the curve fit. It was found in the two-dimensional wall jet studies that the zone of influence of the collision is on the order of two characteristic length scales D. As in that case, there is still some evidence of the turning of the flow at $X/D = 2$. The residual velocities shown in the tails of the velocity distribution are similar to those found previously. This entrainment flow is also very evident in the smoke flow-visualization studies (Fig. 6). The mean velocity profiles are symmetric. These similarity profiles may be expressed as $U/U_{max} = \exp\{-0.693\,\eta^2\}$ where $\eta = Y/B$. The constants in the curve fits have been absorbed into the virtual origin shift. The virtual origin is about -2.65 X/D from the collision point. The mixing-layer growth rate is about twice the free jet value. The similarity profile for this flow can be written as $U/U_{max} = \exp[-12.0\,(Y/X)^2]$ where the free jet coefficient is between 70.7 and 75.0. Since the mixing-layer growth rate is higher, conservation of momentum demands that the mean velocity decay must be correspondingly lower. Our decay curve is $U_{max}/U_0 = 1.5/(X/D)$ compared to a coefficient of about 3.5 in the free jet case.

The mass flow rate at any point may be given by

$$\frac{Q}{Q_{CL}} = \frac{\int U 2\pi X \mathrm{d}_y}{U_{CL} D X_{CL} 2\pi F} = C\left(\frac{X}{D}\right)$$

where the denominator represents the mass flow at the centerline from a single wall jet. Using the empirical data at the centerline gives $C = 0.177$ and the entrainment velocity $\alpha_e = 0.27$. This is more than twice the 0.12 value found in free radial jets. In the two-dimensional upwash case, the entrainment rate was 0.125 of the local maximum, which is 2.4 times a two-dimensional free jet. The entrainment velocity represents only the magnitude of the velocity-carrying mass into the upwash and is not expected to appear strictly as a transverse velocity component. The momentum coefficient may be computed from

$$\frac{J}{J_0} = \frac{\int U^2 X \mathrm{d}_y}{U_0^2 R G} = C_2$$

which is a constant. Although there are some errors in assumptions and calculation of shape factors, evidently they must be compensating because evaluating the foregoing constant with our data gives the constant = 1.01.

In addition to growth rate, another significant departure from free jet characteristics is found in the intermittency. Figure 11 shows the normalized intermittency. The intermittency is determined by the flatness factor normalized by the centerline value. An intermittency factor of one indicates fully turbulent flow. In all free shear flows, the ratio of the intermittency half-width to mean velocity half-width is two.[12] Our measurements in the upwash give this ratio as one. There is evidence[1] that a radial free jet intermittency will continue to erode the core for a greater distance downstream. The data here show the intermittency structure to be established rapidly and be maintained downstream. All profiles of turbulent quantities are normalized by local mean velocity half-widths. Therefore, although the form of these profiles will look absolutely correct (i.e., like a free radial jet), the widths of the profiles actually will be about twice the free jet widths. Since the intermittency profile does not have a flat region at the centerline, the nonturbulent flow outside the upwash is penetrating nearly to the centerline; that is, the mixing layer must have a penetration length scale nearly equal to the half-velocity width. An indication of the size of these eddies compared to a wall jet, for example, can be clearly seen in the flow-visualization photographs.

Figure 12 shows the total turbulence kinetic-energy profile at six measurement stations. Similarity is reached at about $X/D = 4$, which is much faster than usually found in radial free jets and is about the same found for the two-dimensional

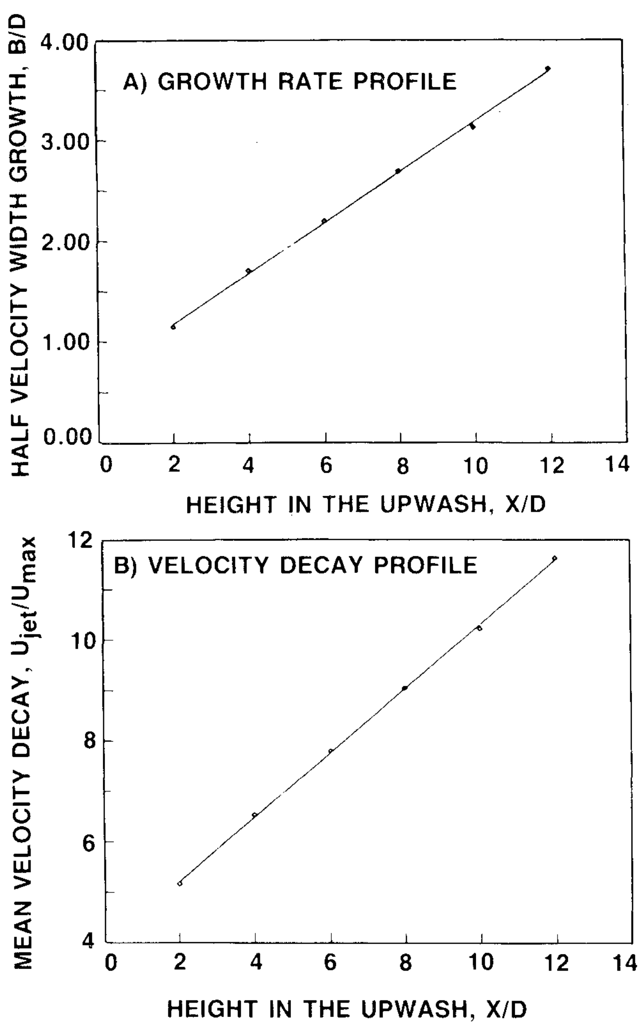

Fig. 9 Radial upwash characteristics along the centerline.

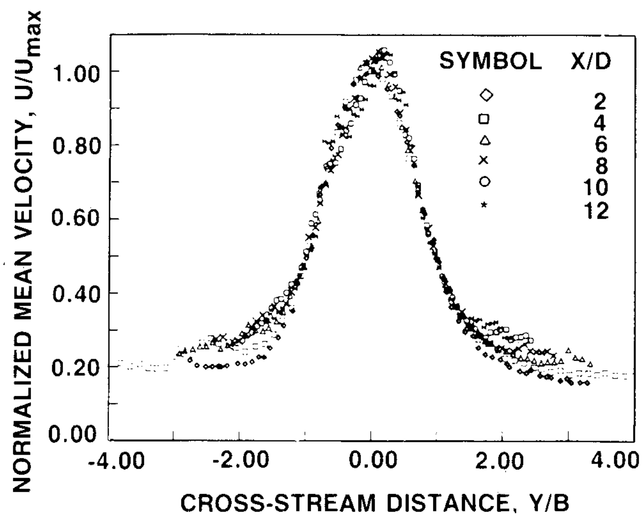

Fig. 10 Normalized mean velocity profiles.

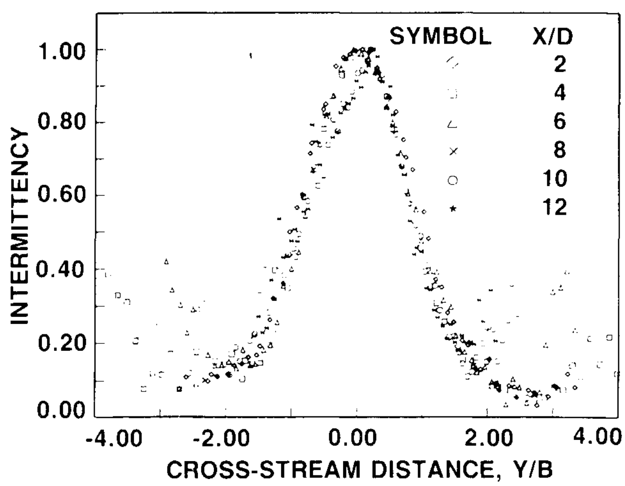

Fig. 11 Intermittency profiles.

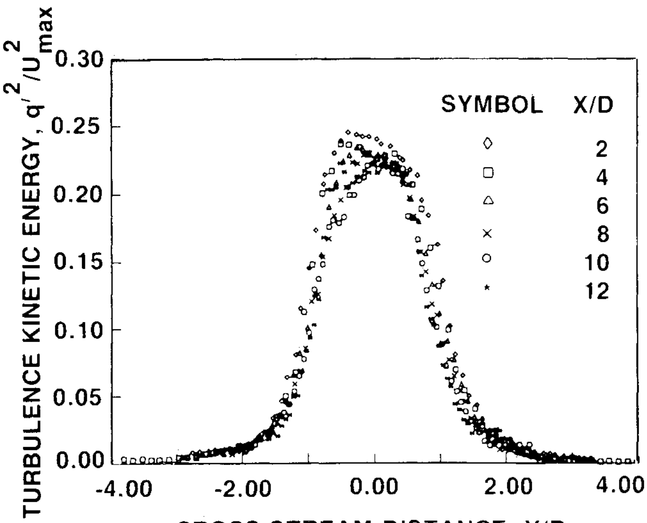

Fig. 12 Total turbulence kinetic energy.

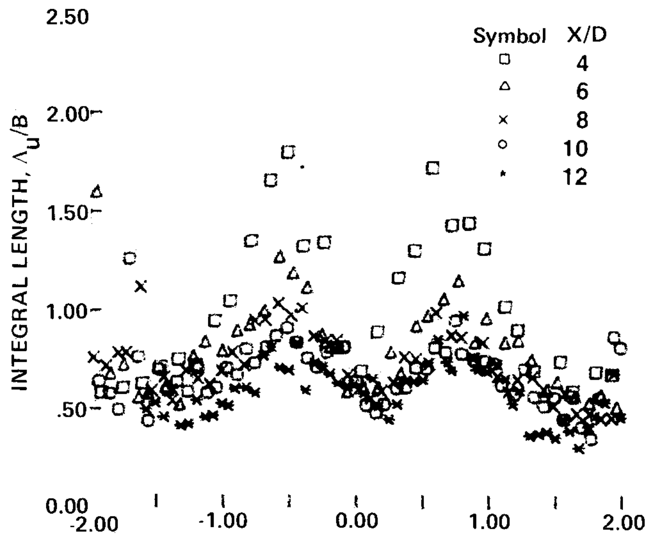

Fig. 13 Integral scale lengths.

upwash. This may be due to the fact that there is no core region that needs to decay before the similarity jet can form. The forms of these profiles are exactly those expected to be found in a radial free jet, but the magnitudes are about 10% high.

Information about the influence of a turbulent fluctuation on its surroundings can be found by examining the autocorrelation of the original time series. The autocorrelation, at a point, of a time series using Taylor's hypothesis can be thought of as a measure of the physical extent of the influence of a fluctuation. A measure of this quantity then gives an idea of the length of mixing involvement. The integral length scale is defined as the integral under the autocorrelation curve. The integral scale lengths were obtained by integrating the area under the autocorrelation curve to the point of the first zero crossing. Since the autocorrelation is also the inverse Fourier transform of the power-spectral density function, it does not give any additional information about the flow. However, it does give another physical interpretation to the length scales identified in the spectral representation.

It is apparent from the length scale profile shown in Fig. 13 that the large-scale eddies at the half-width position are nearly as large as the upwash width itself. Through the center region, it is seen that these eddies are a significant percentage of the

Table 1. Summary of parameters off the centerline

Z/D	Growth rate	Decay rate	Mass coefficient	Entrainment rate	Momentum coefficient
0	0.252	0.638	0.177	0.269	1.01
2	0.230	0.609	0.169	0.245	1.01
4	0.222	0.605	0.165	0.236	0.99
6	0.195	0.561	0.156	0.208	1.01
−2	0.250	0.654	0.172	0.266	0.95

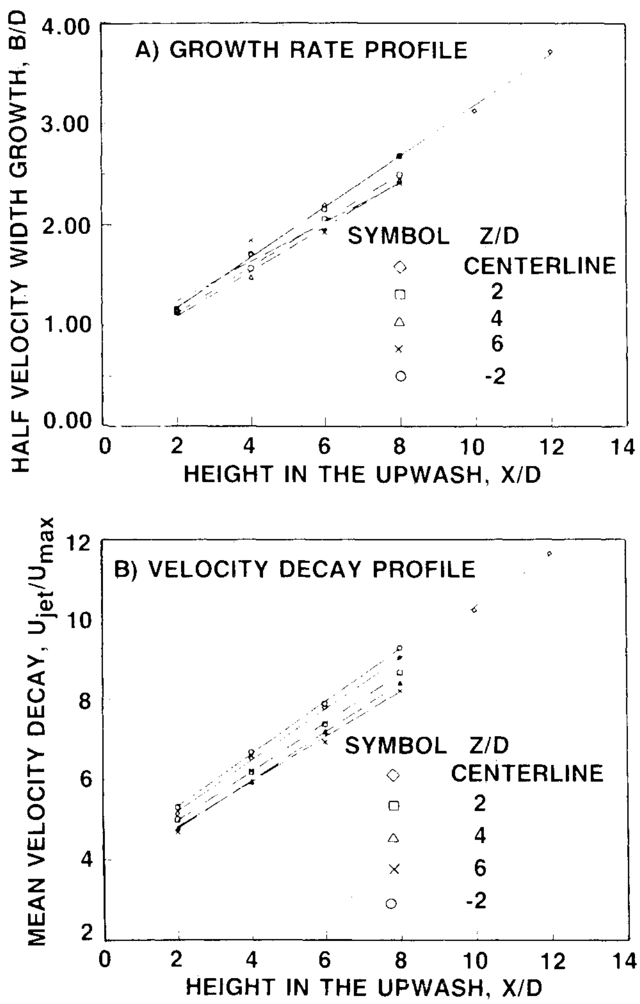

Fig. 14 Radial upwash character.

local mean velocity half-width. The eddies are much larger than those found in a free jet flow, again by a factor of two!

Upwash Measurements—Off Centerline

Figure 8 shows the positions used for off centerline measurements. Only means, turbulence energy, and one Reynolds stress component were obtained for each of two orientations of the X probe. The results are similar to those already presented in the centerline plane connecting the source jets. Measurements were made through the upwash on four planes parallel to the centerline plane. These planes were at positions $2D$, $4D$, $6D$, and $-2D$ with respect to the centerline plane. All the statistics were computed as before.

The half-velocity growth rate for each set of data is shown in Fig. 14a. The slightly slower growth rate that is seen farther away from the centerline occurs because the flow has traveled a farther distance from the origin by the time it gets to each height and, therefore, has had longer to decay. This can be seen in Fig. 1. At $\pm 2D$ the effect is small. However, for $Z/$

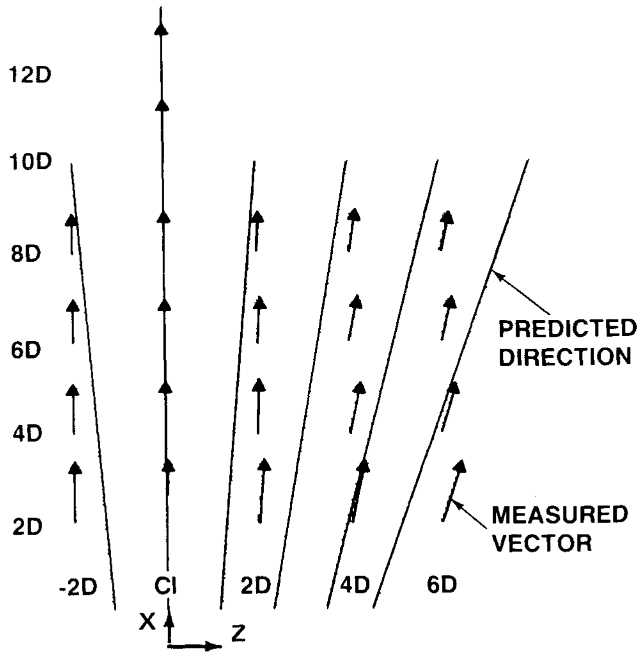

Fig. 15 Measured and predicted velocity vectors in the symmetry plane.

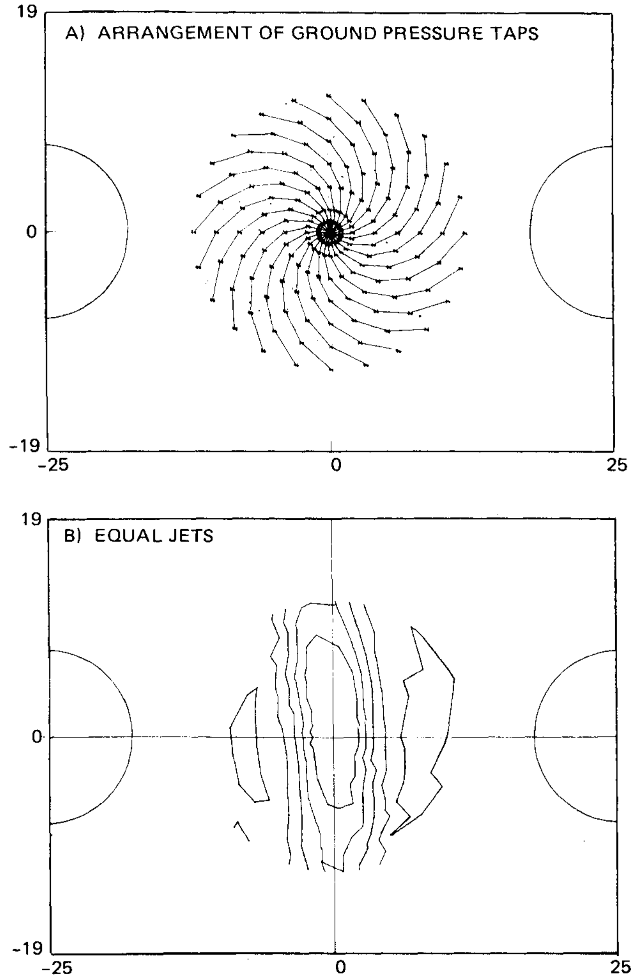

Fig. 16 Ground plane pressure contour.

$D = 6$, the measurement station is as much as $1.8D$ farther downstream from the virtual origin than the equivalent position in the centerline. The growth rate decreases from a maximum of 0.25 at the centerline to 0.20 six characteristic dimensions outboard.

Figure 14b shows the linear decay rates. The lower maximums at any height away from the centerline are very apparent. Although the values are lower, the rates as shown by the slope of the curves are almost constant. Important empirical parameters are summarized in Table 1.

Because measurements were made using an X probe, mean velocities V and W also were obtained with no directional ambiguity. Although the two source radial jets were set in every way similar, a slight preference of the upwash sheet to bend to one side was seen in the V mean data. This is the direction connecting the source jets. The magnitude of this velocity component decreased rapidly with height above the ground. The maximum at the lowest station was less than 15% of the local mean velocity in the X or upwash direction. This represents a slight variation in flow angle from vertical of less than 10 deg. The two-dimensional wall jet upwash flows did not have this type of behavior.

The flow in the symmetry plane was measured separately with the X probe traversed along the plane. From these data, it is possible to compute the velocity vector in the plane perpendicular to the line connecting the source jets. The theory derived from a simple conservation criterion requires that all of these vectors are straight and emanate from the same virtual origin. The measured values with the theoretical prediction for the symmetry are shown in Fig. 15. To the positive Z side, the agreement is very good. On the negative side, the vectors seem to point more closely to the vertical. The vectors turn more toward the vertical as you go away from the symmetry plane. This is reasonable since this flow is more influenced by entrainment and less by direct collision with the opposing wall jet. The reason that the negative side vectors are different from the positive is a small wrinkle in the upwash fan. Throughout the initial stages of setting up this experiment, it was continuously re-emphasized that even a small variation in the wall jet profiles along the collision line would result in a slanting or wrinkling of the upwash fan.

Ground Plane Pressures

A rotating plate in the center of the ground instrumentation plate allowed us to measure ground pressures. The circular plate had eight pressure taps located at the centerline and at 1, 2, 4, 6, 8, 10, and 12 cm in a log spiral arrangement as shown in Fig. 16a. The taps were connected to a scanivalve. The plate was rotated to a position, and the scanivalve was activated with enough time delay for the transconductance transducer to acquire the next pressure. The plate was moved in 15 deg increments to 24 locations. The first and last positions are the same to test for drift. This gives $7 \times 24 = 168$ unique pressure points over a 24 cm diameter circle from a point centered between the source jets.

A contour plot for an equal radial wall jet pressure is shown in Fig. 16b. The contour lines shown are for values of static presure equal to 0.0, 0.2, 0.4, 0.6, and 0.8 of the centerline pressure. Values of 0.0 are possible because there are places where the pressure actually goes negative with respect to ambient pressure far away from the collision zone. All contours close eventually, but sometimes outside of the tap hole range shown in Fig. 16a. The centerline pressure reached a value that exceeds the value corresponding to the complete conversion of a single radial wall jet mean velocity to a total pressure by 47.5%. That is, simply bringing the wall jet to an isotropic stop does not account for the large increase in ground plane static pressure. Most of this static pressure seems to be recovered by accelerating the flow vertically. The pressure rise is primarily responsible for the momentum redistribution.

Conclusions

An experimental investigation of the turbulence mechanisms in a V/STOL upwash flowfield was conducted. A comprehensive data base has been generated for the upwash flow formed from the collision of radial wall jets. These results provide detailed data on an important class of flows where none existed and are expected to significantly improve the computational empirical tools available for predicting V/STOL behavior near the ground.

A new flow facility was constructed to simplify the geometric complexity and interference effects found in a real V/STOL flow. The facility generates two equal radial wall jets by impinging a pipe flow onto a circular deflection plate from below the ground plane. Extensive measurements were made on the resulting radial wall jet to assure that the flow characteristics were the same as generated by more conventional means.

The upwash flow very rapidly becomes self-preserving. If we use the collision point half-velocity height as a characteristic dimension, the flow is self-preserved by X/D about 4. Required linear relationships for mean velocity decay and growth rate were found at all stations across the upwash. Conservation of momentum was observed. A simple model of the upwash using a free jet equivalent may appear adequate on the symmetry plane, but it underpredicts decay rate and fails completely away from the symmetry plane. The basic turbulence characteristics in the upwash formed from the collision of radial wall jets are similar to but about 10% higher than those in a radial free jet. Comparisons suffer from lack of good radial free jet data. The most notable differences are found in the much greater mixing-layer growth rate (and corresponding mean velocity decay rate) and turbulence scale. The mixing rate (0.25) is more than twice that for the free jet case (0.11), which is already greater than a two-dimensional free jet case (0.09). This means that there is a very large entrainment field as seen in the flow visualization. A unique feature of the entrainment is the suckdown into the collision zone rather than a tangential injection. Measurements of the length scale, flow visualization, and most obviously the intermittency show the unusually large structure of the upwash.

The higher mixing rate can be explained primarily by the head-on collision of the wall jets. This creates large turbulent eddies that involve more ambient fluid than a simple jet emanating from a slot. This also is seen by the large static-pressure field at the collision point. Since the intermittency function extends more into the core of the upwash flow, time-averaged turbulence energy that has approximately the same value as a free jet must be more energetic when it is present.

Acknowledgments

This research was funded by the Air Force Office of Scientific Research under Contract No. F49620-85-C-0111 by Dr. James Wilson.

References

[1]Rajaratnam, N., *Turbulent Jets, Developments in Water Science*, 5th ed., Elsevier, Amsterdam, 1976.

[2]Kind, R. J. and Suthanthiran, K., "The Interaction of Two Opposing Plane Turbulent Wall Jets," AIAA Paper 72-211, Jan. 1972.

[3]Witze, P. O. and Dwyer, H. A., "Impinging Axisymmetric Turbulent Flows: The Wall Jet, the Radial Jet and Opposing Free Jets," *Proceedings of the Symposium on Turbulent Shear Flows*, Vol. 1, Univ. of Pennsylvania Press, University Park, PA, April 1977.

[4]Kotansky, D. R. and Glaze, L. N., "The Effects of Ground Wall-Jet Characteristics on Fountain Upwash Flow Formation and Development," AIAA Paper 81-1294, June 1981.

[5]Foley, W. H. and Finley, D. B., "Fountain Jet Turbulence," AIAA Paper 81-1293, June 1981.

[6]Jenkins, R. A. and Hill, W. G., Jr., "Investigation of VTOL Upwash Flows Formed by Two Impinging Jets," Grumman Corporate Research Center, Bethpage, NY, Rept. RE-548, Nov. 1977.

[7]Saripalli, K. R., "Laser Doppler Velocimeter Measurements in 3-D Impinging Twin-Jet Fountain Flows," AIAA Paper 85-4037, Oct. 1985.

[8]Gilbert, B. L., "Detailed Turbulent Measurements in a Two-Dimensional Upwash," AIAA Paper 83-1678, July 1983.

[9]Gilbert, B. L., "An Investigation of Turbulence Mechanisms in V/STOL Upwash Flow Fields," Grumman Research and Development Center, Bethpage, NY, Rept. RE-708, Sept. 1985.

[10]Gilbert, B. L., "An Investigaion of Turbulence Mechanisms in V/STOL Upwash Flow Fields," Grumman Research and Development Center, Bethpage, NY, Rept. RE-730, March 1987.

[11]Gilbert, B. L., "Turbulence Measurements in a Flow Generated by Colliding Radial Wall Jets," *Experiments in Fluids,* (submitted for publication).

[12]Townsend, A. A., *The Structure of Turbulent Shear Flow,* 2nd ed., Cambridge Univ. Press, Cambridge, England, UK, 1980.